

# Dynamic control of the photonic band gap using quantum coherence

X. M. Su<sup>1,2</sup> and B. S. Ham<sup>1</sup>

<sup>1</sup>Graduate School of Information and Communications, Inha University, Incheon 402-715, Korea

<sup>2</sup>College of Physics, Jilin University, Changchun 130023, People's Republic of China

(Received 29 July 2004; published 31 January 2005)

We propose a scheme of employing quantum interference and coherence in an optical medium with coupled electromagnetic fields to create a photonic band gap. A variable photonic band gap is achieved by the cross-phase-modulation of two counterpropagating coupling fields on a weak probe pulse. The proposed photonic band gap has potential applications for the dynamic control of group velocity dispersion compensation in fiber-optic communications.

DOI: 10.1103/PhysRevA.71.013821

PACS number(s): 42.65.Re, 42.70.Qs, 42.50.Gy

Quantum coherence and interference in an optical medium interacting with radiation fields have led to interesting coherent effects such as electromagnetically induced transparency (EIT) [1], slow and frozen light [2,3], squeezed-light generation [4], optical phase conjugation [5], photonic switching [6], quantum coherence swapping [7], and electromagnetically induced gratings [8,9]. Quantum interference between quantum transition pathways can lead to a substantial modulation of the absorption and dispersion properties of an optical medium. Recently, Lukin and co-workers demonstrated photon localization using a standing wave grating based on EIT [3,10], and Xiao and co-workers demonstrated photonic gratings by applying EIT to the grating diffraction theory [8,9]. These results make use of the optical properties of the induced transparency of a probe at resonance frequency.

Here, we propose a scheme that employs quantum interference and coherence in an optical medium and external electromagnetic fields to create a photonic band gap. The periodic refractive-index modulation of the medium resulting from the quantum coherence and interference leads to the creation of a photonic band gap, which is dynamically controllable. In particular, this photonic band gap can be applied to broadband optical filters with high resolution, high-speed optical switches, and dispersion compensators in fiber-optic communications, which are bandwidth limited in conventional optical device technologies, for the purpose of achieving dynamic control.

A pair of counterpropagating strong coupling fields at frequency  $\omega_c$  with an identical Rabi frequency of  $\Omega_c$  can create a standing wave grating in an optical medium by inducing refractive-index change of the medium (see Fig. 1). The amplitude of the standing wave grating is proportional to  $\Omega_c \cos(k_c z)$ , where  $k_c$  is a propagation vector of the fields, and the standing wave period is  $2\pi/k_c$ . Under the action of the standing wave grating, a weak probe pulse at frequency  $\omega_p$  with propagation vector  $k_p$  propagating through the medium has been demonstrated to be completely blocked [3,10] and efficiently deflected [8,9]. In Fig. 1, the frequency of the probe field  $\omega_p$  is near resonant to the transition  $|2\rangle - |1\rangle$  with a detuning  $\Delta_2$ :  $\Delta_2 > \Omega_c, \gamma_2$ , where  $\gamma_2$  is the optical decay rate. The reason for the detuning of the probe in Fig. 1 is to avoid any absorption and to maximize transmission. The coherent

interactions of the standing wave fields and the probe pulse with the corresponding optical transitions in Fig. 1 can create a photonic band gap under certain conditions. Here, it must be noted that the creation of the photonic band gap has nothing to do with EIT, because the probe frequency is greatly detuned from the resonance frequency, and the condition of two-photon resonance is never satisfied. In the proposed photonic band gap, the counterpropagating coupling fields form a standing wave grating causing coherent polarization modulation of the medium at a frequency close to that of the probe field. We emphasize that our scheme is not the same as conventional fiber Bragg gratings, where the grating parameters are fixed for the probe frequency selection [11]. Instead, in the present scheme of a photonic band gap employing interactions of the coupling and probe fields with an optical medium, the grating parameters can be dynamically controllable by simply adjusting the frequency detuning and the Rabi frequency of the coupling fields.

Here we introduce the cross-phase-modulation (XPM) effects of the two coupling fields acting on a weak probe pulse. In a conventional ladder-type three-level XPM scheme [12], only one coupling field is needed. Coherence interaction between the coupling and the probe create refractive-index changes as usual. The phase shift experienced by the probe depends on the third-order nonlinear susceptibility  $\chi^{(3)}$ , which is maximized at resonance frequency. To avoid absorption, however, the probe field must be detuned from the line center, so that  $\chi^{(3)}$  is generally very small. Thus, this nonlinear refractive-index modulation by traditional method has a very small effect on the group velocity dispersion compensation.

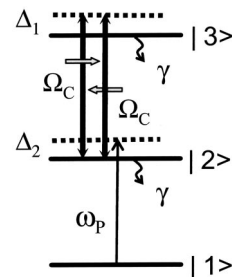


FIG. 1. Schematic of a photonic band gap induced by quantum interference.

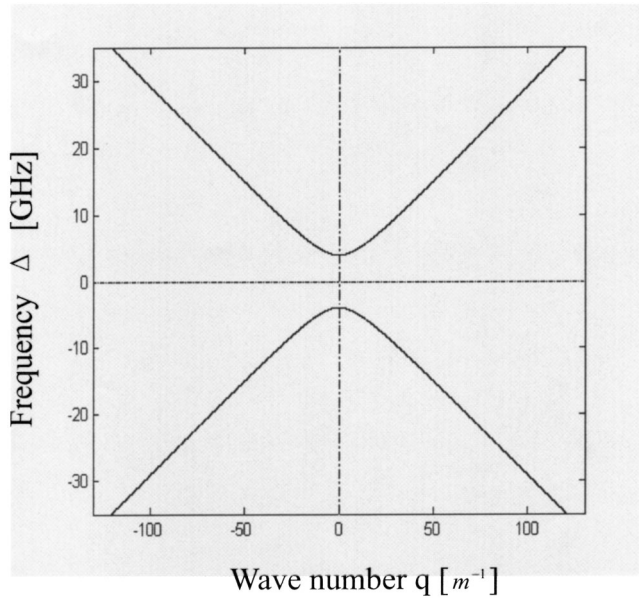


FIG. 2. Illustration of the dispersion relation of a band gap in  $\text{Er}^{3+}$ . The resonant frequencies of the coupling and the probe fields are  $5904$  and  $6595 \text{ cm}^{-1}$ , respectively. The two-photon detuning is  $\Delta_1 + \Delta_2 = 0.1 \text{ MHz}$ ; the Rabi frequency of the coupling field is  $|\Omega_c| = 50.0 \text{ MHz}$ ;  $\mu_{21}^2 N / \hbar \epsilon_0 = 5 \times 10^{12} \text{ s}^{-1}$ .

To overcome such a low  $\chi^{(3)}$ , EIT techniques have been applied for giant Kerr nonlinearity by tuning the probe to resonance frequency [12]. Even though the giant Kerr nonlinearity induced by EIT is several orders of magnitude larger in  $\chi^{(3)}$  and causes the probe pulse to experience a  $\pi$  phase shift [4], satisfying EIT conditions in solid or semiconductor bulk media is not so easy due to intrinsically large inhomogeneous broadening. In this paper, we suggest a technique of photonic-band-gap creation based on off-resonance counterpropagating fields as shown in Fig. 1. The quantum coherence between a standing wave made by the counterpropagating coupling fields and the probe field leads to refractive-index change. According to the coupled wave equations, Fig. 1 reaches a photonic band gap which prohibits the probe pulse propagation. At the edge of the band gap, however, the probe pulse experiences a sharp dispersion change (which will be discussed later in Fig. 2), and therefore we can control the group velocity dispersion of the probe. Here we should mention that we use the linear properties of the matter-field interactions for demonstration of the dynamic photonic band gap.

In Fig. 1, the counterpropagating coupling fields induce periodic refractive-index change in the medium. Under this condition of modified refractive index a probe field  $E_p$  can be decomposed into two slowly varying amplitudes,  $\epsilon_+(z)$  for the forward direction and  $\epsilon_-(z)$  for the backward direction due to reflections on the grating:  $E_p(z, t) = \frac{1}{2}[(\epsilon_+ e^{ik_p z} + \epsilon_- e^{-ik_p z})e^{-i\omega_p t} + (\epsilon_+ e^{-ik_p z} + \epsilon_- e^{ik_p z})e^{i\omega_p t}]$ . In an interaction picture, the interaction Hamiltonian is expressed as follows in the Hilbert space spanned by the bare states  $|1\rangle$ ,  $|2\rangle$ , and  $|3\rangle$  with the rotational wave approximation:

$$H'_1 = -\hbar[g(\epsilon_+ e^{ik_p z} + \epsilon_- e^{-ik_p z})e^{-i\Delta_2 t}|2\rangle\langle 1| + 2\Omega_c \cos(k_c z)e^{-i\Delta_1 t}|3\rangle\langle 2| + \text{H.c.}], \quad (1)$$

where  $2\hbar g$  is a dipole moment matrix element for the atomic transition  $|2\rangle - |1\rangle$ ;  $\Delta_1 = \omega_c - \omega_{32}$  and  $\Delta_2 = \omega_p - \omega_{21}$  are the frequency detunings of the coupling and the probe fields, respectively. The response of the macroscopic medium to the field is governed by the density-matrix equation [13]:

$$\frac{\partial \rho}{\partial t} = -\frac{i}{\hbar}[H'_1, \rho] + \Lambda \rho, \quad (2)$$

where  $\rho$  stands for the density-matrix operator, and  $\Lambda \rho$  represents all the effects caused by the interactions of atoms with fluctuations. Due to the rotating wave approximation we can obtain newly defined density-matrix elements [8]

$$\sigma_{21} = e^{-i\Delta_2 t} \rho_{21}, \quad \sigma_{31} = e^{-i(\Delta_1 + \Delta_2)t} \rho_{31}, \quad \sigma_{32} = e^{-i\Delta_1 t} \rho_{32},$$

$$\sigma_{jj} = \rho_{jj} \quad (j = 1, 2, 3).$$

By inserting the above relations and Eq. (1) into Eq. (2), the following equations of motion for the matrix elements are obtained:

$$\dot{\sigma}_{21} = -(\gamma_2 - i\Delta_2)\sigma_{21} + ig(\epsilon_+ e^{ik_p z} + \epsilon_- e^{-ik_p z})(\sigma_{11} - \sigma_{33}) + 2i\Omega_c \cos(k_c z)\sigma_{31}, \quad (3a)$$

$$\dot{\sigma}_{31} = -[\gamma_1 - i(\Delta_1 + \Delta_2)]\sigma_{31} + 2i\Omega_c \cos(k_c z)\sigma_{21} - ig(\epsilon_+ e^{ik_p z} + \epsilon_- e^{-ik_p z})\sigma_{23}, \quad (3b)$$

where  $\gamma_1$  and  $\gamma_2$  are the dephasing rates from level  $|3\rangle$  to  $|1\rangle$  and level  $|2\rangle$  to  $|1\rangle$ , respectively. Here we can make our first approximation by neglecting the last term of Eq. (3b), because the probe field is sufficiently weak compared with the coupling fields, and the population in levels  $|2\rangle$  and  $|3\rangle$  is negligible. Inserting  $\sigma_{11} - \sigma_{33} \cong 1$  into Eqs. (3a) and (3b), we can reach the following matrix form [13]:

$$\dot{R} = -MR + A, \quad (4)$$

where

$$R = \begin{bmatrix} \sigma_{21} \\ \sigma_{31} \end{bmatrix},$$

$$M = \begin{bmatrix} \gamma_2 - i\Delta_2 & -2i\Omega_c \cos(k_c z) \\ -2i\Omega_c \cos(k_c z) & \gamma_1 - i(\Delta_1 + \Delta_2) \end{bmatrix},$$

$$A = \begin{bmatrix} ig(\epsilon_+ e^{ik_p z} + \epsilon_- e^{-ik_p z}) \\ 0 \end{bmatrix}.$$

If the pulse duration of the probe field is much longer than  $|\gamma_2 - i\Delta_2|^{-1}$ , then the condition  $\dot{R} = 0$  is satisfied. Thus, we have  $R = M^{-1}A$ , and

$$\sigma_{21} = \frac{ig(\varepsilon_+ e^{ik_p z} + \varepsilon_- e^{-ik_p z})}{(\gamma_2 - i\Delta_2) + \frac{4|\Omega_c|^2 \cos^2(k_c z)}{[\gamma_1 - i(\Delta_1 + \Delta_2)]}}. \quad (5)$$

It is known that  $\sigma_{21}$  is proportional to the polarization of the medium at the frequency of the probe field. If we choose  $|\Delta_2| \gg \gamma_2$ ,  $|\Delta_1 + \Delta_2| \gg \gamma_1$  and  $|\Delta_1 + \Delta_2| > |\Omega_c|$ , then the condition

$$\left| \frac{4|\Omega_c|^2}{(\gamma_2 - i\Delta_2)[\gamma_1 - i(\Delta_1 + \Delta_2)]} \right| \ll 1$$

is satisfied. Thus, Eq. (5) is simplified as

$$\begin{aligned} \sigma_{21} &= ig(\gamma_2 - i\Delta_2)^{-1} \\ &\times \left[ 1 - \frac{4|\Omega_c|^2}{(\gamma_2 - i\Delta_2)[\gamma_1 - i(\Delta_1 + \Delta_2)]} \cos^2(k_c z) \right] \\ &\times (\varepsilon_+ e^{ik_p z} + \varepsilon_- e^{-ik_p z}). \end{aligned} \quad (6)$$

Equation (6) shows the induced coherence caused by the interactions of the fields with the medium, which oscillates at the frequency of the weak probe field with a modulation  $\cos^2(k_c z)$ . According to the definition of polarization,

$$P(z, t) = \frac{1}{2} \varepsilon_0 E_p [\chi(z, \omega_p) e^{-i\omega_p t} + \text{c.c.}], \quad (7)$$

where  $\chi(\omega_p) = \chi' + i\chi''$ . The real and imaginary parts of  $\chi$  lead to the dispersive and absorptive characteristics of the medium. By performing a quantum average of the dipole moment over an ensemble of homogeneously broadened atoms, we have

$$P(z, t) = 2\hbar g N \sigma_{21} e^{-i\omega_p t} + \text{c.c.} \quad (8)$$

From Eqs. (6)–(8), we can find the real and imaginary parts of the complex susceptibility:

$$\chi' = -\frac{\mu_{21}^2 N}{\hbar \varepsilon_0 \Delta_2} \left[ 1 + \frac{4|\Omega_c|^2}{(\Delta_1 + \Delta_2)\Delta_2} \cos^2(k_c z) \right] = \chi'_0 + \Delta\chi', \quad (9a)$$

$$\begin{aligned} \chi'' &= -\frac{\mu_{21}^2 N}{\hbar \varepsilon_0 \Delta_2} \left[ \frac{\gamma_2}{\Delta_2} + \left( \frac{2\gamma_2}{\Delta_2} + \frac{\gamma_1}{(\Delta_1 + \Delta_2)} \right) \frac{4|\Omega_c|^2}{(\Delta_1 + \Delta_2)\Delta_2} \right. \\ &\quad \left. \times \cos^2(k_c z) \right]. \end{aligned} \quad (9b)$$

From the relationship between refractive index and susceptibility [13], we obtain a modulating refractive index of the proposed scheme:

$$n = n_0 + \Delta n \cos(2k_c z), \quad (10)$$

where

$$n_0 = \left( 1 + \frac{\mu_{21}^2 N}{\hbar \varepsilon_0 |\Delta_2|} \right)^{1/2} \quad \text{and} \quad \Delta n = \frac{1}{2} \frac{(n_0^2 - 1)}{n_0} \frac{|\Omega_c|^2}{|\Delta_2| |\Delta_1 + \Delta_2|}.$$

At the same time, the imaginary part of the refractive index is  $n'' \approx \chi''/2(1 + \chi') \ll n_0$ . Thus, the system can be realized for an index modulation with relatively small absorption. In Eq.

(10), we show that the refractive index of the medium is modulated with a period  $2\pi/k_c$ . Here it should be noted that there are forbidden bands in such a periodic medium. The band gap  $\Delta\omega_{gap}$  is given by [14]

$$\Delta\omega_{gap} = \omega_0 \frac{2}{\pi} \frac{\Delta n}{n}, \quad (11)$$

where  $\omega_0$  is the center frequency of the forbidden band. From Eq. (11), the condition  $\Delta n < n_0$  must be satisfied. For Fig. 1, according to the definition of  $\Delta n$  in Eq. (10), the following condition is required:  $|\Omega_c| < |\Delta_1 + \Delta_2|, |\Delta_2|$ .

Inserting Eq. (10) into the wave equation for a homogeneous medium leads to [14]

$$\left( \frac{\partial^2}{\partial z^2} - \frac{n^2}{c^2} \frac{\partial^2}{\partial t^2} \right) E_p = 0. \quad (12)$$

Using slowly varying envelopes, we derive equations of motion for the forward and backward modes, respectively,

$$i \frac{\partial \varepsilon_+}{\partial z} + i \frac{n_0}{c} \frac{\partial \varepsilon_+}{\partial t} + \kappa e^{-2i\Delta k z} \varepsilon_- = 0, \quad (13a)$$

$$-i \frac{\partial \varepsilon_-}{\partial z} + i \frac{n_0}{c} \frac{\partial \varepsilon_-}{\partial t} + \kappa e^{2i\Delta k z} \varepsilon_+ = 0, \quad (13b)$$

where  $\kappa = (\Delta n/2)k_{p0}$  and  $k_{p0}$  is the center wave number of the probe pulse in vacuum. To remove the exponential factors in Eq. (13), we introduce functions  $F_{\pm}$  by the relations  $\varepsilon_{\pm} = F_{\pm} e^{i\Delta k[\mp z + (c/n_0)t]}$ , and thus

$$i \frac{\partial F_+}{\partial z} + i \frac{n_0}{c} \frac{\partial F_+}{\partial t} + \kappa F_- = 0, \quad (14a)$$

$$-i \frac{\partial F_-}{\partial z} + i \frac{n_0}{c} \frac{\partial F_-}{\partial t} + \kappa F_+ = 0. \quad (14b)$$

$F_{\pm}$  can be written in wave number  $q$  space as [14]

$$F_{\pm} = \int_{-\infty}^{\infty} \tilde{F}_{\pm}(q) e^{i(\omega(q)t \mp qz)} dq. \quad (15)$$

Inserting Eq. (15) into Eqs. (14), the dispersion relation of the scheme is obtained:

$$q^2 = \delta^2 - \kappa^2, \quad (16)$$

where  $\delta = (n_0/c)\omega$ . Typically  $\omega$  and  $q$  are characterized by the center frequency  $\omega_0$  and corresponding wave number  $k_0$ . In our scheme, given that  $\omega_0 = \omega_c$  and  $k_0 = k_c$ ,  $\omega = (\omega_p - \omega_c) = \Delta$  and  $q = k_p - k_c = \Delta k$  when the frequency and the wave number of the coupling field are fixed. The stop band corresponds to the detuned frequencies  $-\kappa < \delta < \kappa$ , where the reflectivity is high. Equation (16) demonstrates the band gap of the proposed photonic-band-gap scheme in Fig. 1. According to Eq. (16), the group velocity of the probe pulse is  $v_g = d\Delta/dq = (c/n_0)(1/\delta)\sqrt{\delta^2 - \kappa^2}$ , and the group velocity dispersion is  $dv_g/d\Delta = \kappa^2/\delta^3\sqrt{1 - \kappa^2/\delta^2}$ .

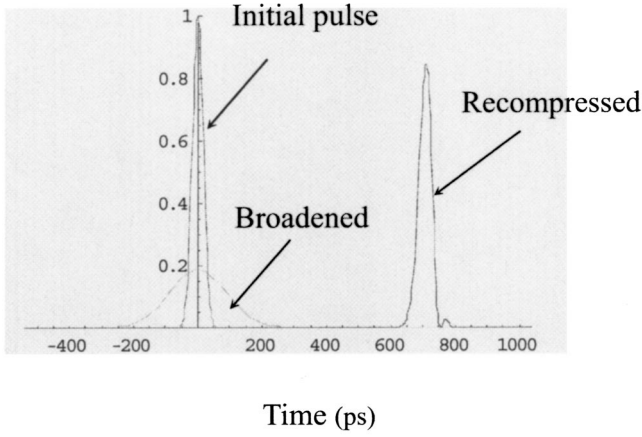


FIG. 3. Numerical demonstration of dispersion compensation. The initial pulse has a Gaussian form with a duration of 40 ps (full width at half maximum). For the broadened pulse, the propagation length of the fiber is 150 km; for the recompressed pulse, the parameters are  $|\Omega_c|=80.0$  MHz,  $\Delta_1+\Delta_2=1.6$  KHz,  $\mu_{21}^2 N/\hbar\epsilon_0=5 \times 10^{12}$  s $^{-1}$ , and  $M_3=0.4$ , and the length of the medium is  $L=1.88$  cm to satisfy the relation  $L_g\beta_2^g+L_f\beta_2^f=0$ .

Using Eq. (16), we now investigate dispersive properties of the probe field. In our scheme, the Rabi frequency  $\Omega_c$  and the frequency detuning  $\Delta_1$  ( $\Delta_2$ ) of the coupling (probe) field determine the band gap:

$$\Delta n = \frac{1}{2} \frac{(n_0^2 - 1)}{n_0} \frac{|\Omega_c|^2}{|\Delta_2||\Delta_1 + \Delta_2|}.$$

With the definition  $\Delta = \omega_p - \omega_c$ , we can derive  $\Delta_2 = \Delta + \Delta_1 + (\omega_{32} - \omega_{21})$ , where  $\Delta_2$  can be large, even though  $\omega_p \sim \omega_c$ . Thus, the dynamic control of the band gap  $\Delta\omega_{\text{gap}}$  [Eq. (11)] is possible by adjusting the optical parameters in the  $\Delta n$ .

To numerically prove the proposed photonic band gap, we choose fluorozirconate glass doped with Er $^{3+}$  ions [15] as an optical medium. The three energy levels  $^4I_{15/2}$ ,  $^4I_{13/2}$ , and  $^4I_{9/2}$  of Er $^{3+}$  ions are chosen for the states |1>, |2>, and |3> in Fig. 1. By solving Eq. (16) directly with proper optical parameters, we can plot a dispersion relation. Figure 2 shows photonic-band-gap creation. We find that the optical dispersive properties of the medium are modulated by the two coupling fields near the edge of the band gap ( $\delta = \kappa$ ). Far away from the band edges, the group velocity and its dispersion are the same as they were without the two coupling fields. At the band edges the group velocity of the probe reaches exactly zero. This demonstrates that a probe pulse is trapped in the medium, where its frequency is determined by  $\delta = \kappa$ . It is already known that the group velocity dispersion near the edges of the band is several orders of magnitude larger than that of the bare fibers [11]. The sign of the group dispersion of the lower branch of the curves in Fig. 2 is negative, and can thus be used to compensate anomalous dispersion effects in optical fiber transmission [11]. Therefore, the dispersion compensation becomes a direct application of the proposed photonic-band-gap scheme.

For a numerical simulation of the dispersion compensation (see Fig. 3), we assume that the probe pulse has a Gauss-

ian envelope with a duration  $\tau_{\text{FWHM}}=40$  ps. The probe pulse propagates through a 150-km-long optical fiber at a central wavelength of 1.55  $\mu\text{m}$ . Because of the second dispersion of the fiber,  $\beta_2^f=-20$  ps $^2$ /km, the probe pulse should be broadened to 208 ps as it travels through the fiber [16]. The broadened probe pulse has the form  $E_f(L_f, t) = \int_{-\infty}^{\infty} U(0, \omega) \exp[(i/2)\beta_2^f \omega^2 L_f - i\omega t] d\omega$ , where  $U(0, \omega)$  is the Fourier transform of the initial pulse at  $z=0$ . We allow the broadened probe pulse to now enter the Er photonic-band-gap medium for proof of the present technique of pulse compensation. The output pulse should have the following form:

$$E_f(L_f + L_g, t) = \int_{-\infty}^{\infty} U(0, \omega) \exp\left(\frac{i}{2}\beta_2^f \omega^2 L_f + \frac{i}{2}\beta_2^g \omega^2 L_g + \frac{i}{6}\beta_3^g \omega^3 L_g - i\omega t\right) d\omega.$$

Here  $L_g$  ( $L_f$ ),  $\beta_2^g$  ( $\beta_2^f$ ),  $\beta_3^g$  are the grating (fiber) length, the second order of the grating (fiber) dispersion, and the third order of the grating dispersion, respectively. In order to compress the pulse using the dispersion compensation, the condition  $L_g\beta_2^g+L_f\beta_2^f=0$  must be satisfied [16]. At the same time, the third- and higher-order dispersion parameters should be as small as possible to avoid recompression distortion. For the numerical calculations, we introduce a merit parameter  $M_3=0.4$  to prevent the recompressed pulse from being distorted, where  $M_3$  is the ratio of the third-order dispersion to the second-order dispersion.

For a specific example of the present idea, we can choose the following reasonable parameters: the coupling laser diode power is at 10 mW; the dipole matrix element  $\mu_{21}$  is estimated in the order of  $10^{-29}$  cm [15,17,18]; then the Rabi frequency of the 10-mW coupling laser reaches a few gigahertz if the fiber core diameter is a few micrometers. Because the probe frequency  $\omega_p$  must be 6451 cm $^{-1}$  (from the wavelength of 1.55  $\mu\text{m}$ ) to satisfy the communication wavelength, the detuning of the probe must be  $\Delta_2 = 540$  cm $^{-1}$  ( $\Delta_2 = \omega_p - \omega_{21}$ ). In order to get the appropriate grating parameter  $\kappa$  to compress the pulse broadening down to the initial one, the two-photon detuning  $\Delta_1 + \Delta_2$ , which is near resonant to  $\omega_{31}$  in Fig. 1, must be determined by Eq. (10).

Figure 3 shows each field evolution in time for the initial probe pulse, for the broadened pulse after propagation through a dispersive medium, and for the recompressed pulse due to the dispersion compensation. We depict Fig. 3 using the permitted parameters discussed above. We note that the peak intensity of the recompressed pulse in Fig. 3 is near 85% of its initial value. The estimated energy loss of the recompressed pulse is 0.13% of the initial pulse. The small tail of the recompressed pulse near 800 ps in Fig. 3 results from the nonzero third dispersion term. Therefore, Fig. 3 demonstrates that pulse broadening through a dispersive medium can be remarkably compensated by the two coupling fields in the present dynamic photonic-band-gap scheme.

In conclusion, we have proposed and numerically demonstrated a dynamically controllable photonic band gap using quantum interference and coherence. We have also shown

one example of the proposed band-gap theory for a pulse compression with group velocity dispersion compensation. The proposed technique using counterpropagating electromagnetic fields has potential for dispersion compensators [19] and frequency filters in dense-wavelength-division-multiplexing fiber-optic communications [20]. Compared with conventional (passive) fiber Bragg gratings whose

frequency selection is fixed, the present technique has the advantage of dynamic control of the band gap with linear control of the control laser parameters.

This research was supported by Korea Research Foundation Grant No. KRF-2003-070-C00024.

- 
- [1] S. E. Harris, *Phys. Today* **50** (7), 36 (1997); K. J. Boller, A. Imamoglu, and S. E. Harris, *Phys. Rev. Lett.* **66**, 2593 (1991); Y. Zhao, C. Wu, B. S. Ham, M. K. Kim, and E. Awad, *ibid.* **79**, 641 (1997); B. S. Ham, M. S. Shshriar, and P. R. Hemmer, *Opt. Lett.* **22**, 1138 (1997); J. Faist, F. Capasso, C. Sirtori, K. W. West, and L. N. Pfeiffer, *Nature (London)* **390**, 589 (1997); G. B. Serapiglia, E. Paspalakis, C. Sirtori, K. L. Vodopyanov, and C. C. Phillips, *Phys. Rev. Lett.* **84**, 1019 (2000); M. Phillips, H. Wang, I. Romyantsev, N. H. Kwong, R. Takayama, and R. Binder, *ibid.* **91**, 183602 (2003).
- [2] Lene Vestergaard Hau, S. E. Harris, Zachary Dutton, and Cyrus H. Behroozi, *Nature (London)* **397**, 594 (1999); M. M. Kash, V. A. Sautenkov, A. S. Zibrov, L. Hollberg, G. R. Welch, M. D. Lukin, Yu. Rostovtsev, E. S. Fry, and M. O. Scully, *Phys. Rev. Lett.* **82**, 5229 (1999); C. Liu, Z. Dutton, C. F. Behroozi, and L. V. Hau, *Nature (London)* **409**, 490 (2001); D. F. Phillips, A. Fleischhauer, A. Mair, R. L. Walsworth, and M. D. Lukin, *Phys. Rev. Lett.* **86**, 783 (2001); A. V. Turukhin, V. S. Sudarshanam, M. S. Shahriar, J. A. Musser, B. S. Ham, and P. R. Hemmer, *ibid.* **88**, 023602 (2002).
- [3] M. Bajcsy, A. S. Zibrov, and M. D. Lukin, *Nature (London)* **426**, 638 (2003).
- [4] M. D. Lukin, A. B. Matsko, M. Fleischhauer, and M. O. Scully, *Phys. Rev. Lett.* **82**, 1847 (1999).
- [5] P. R. Hemmer, D. P. Katz, J. Donoghue, M. Cronin-Golomb, M. S. Shahriar, and P. Kumar, *Opt. Lett.* **20**, 982 (1995); Y. Li and M. Xiao, *ibid.* **21**, 1046 (1996).
- [6] S. E. Harris and Y. Yamamoto, *Phys. Rev. Lett.* **81**, 3611 (1998); A. Imamoglu, H. Schmidt, G. Woods, and M. Deutsch, *ibid.* **79**, 1467 (1997).
- [7] B. S. Ham and P. R. Hemmer, *Phys. Rev. Lett.* **84**, 4080 (2000).
- [8] Hong Yuan Ling, Yong-Qing Li, and Min Xiao, *Phys. Rev. A* **57**, 1338 (1998).
- [9] Masaharu Mitsunaga and Nobuyuki Imoto, *Phys. Rev. A* **59**, 4773 (1999); G. C. Cardoso and J. W. R. Tabosa, *ibid.* **65**, 033803 (2002).
- [10] A. Andre and M. D. Lukin, *Phys. Rev. Lett.* **89**, 143602 (2002).
- [11] N. M. Litchinitser, B. J. Eggleton, and D. B. Patterson, *J. Lightwave Technol.* **15**, 1303 (1997).
- [12] H. Schmidt and A. Imamoglu, *Opt. Lett.* **21**, 1936 (1996).
- [13] M. O. Scully and M. S. Zubairy, *Quantum Optics* (Cambridge University Press, Cambridge, U.K., 1997).
- [14] A. Yariv and P. Yeh, *Optical Waves in Crystals* (Wiley Interscience, New York, 2003).
- [15] M. D. Shinn and W. A. Sibley, *Phys. Rev. B* **27**, 6635 (1983).
- [16] Govind P. Agrawal, *Nonlinear Fiber Optics* (Academic, New York, 1995).
- [17] E. Desurvire, *J. Lightwave Technol.* **8**, 1517 (1990).
- [18] M. Janos and S. C. Guy, *J. Lightwave Technol.* **16**, 542 (1998).
- [19] N. M. Litchinitser, B. J. Eggleton, and G. P. Agrawal, *J. Lightwave Technol.* **16**, 1523 (1998).
- [20] K. P. Jones, M. S. Chaudhry, L. Simeonidou, N. H. Taylor, and P. R. Morkel, *Electron. Lett.* **31**, 2117 (1995).